OPTICAL REVIEW Vol. 13, No. 6 (2006) 417–423

Gradient-Based Blind Deconvolution with Phase Spectral Constraints

Noriaki SUETAKE*, Morihiko SAKANO[1] and Eiji UCHINO

Academic Domain of Natural Science, Graduate School of Science and Engineering, Yamaguchi University, 1677-1 Yoshida, Yamaguchi 753-8512, Japan

[1]*Division of Natural Science and Symbiosis, Graduate School of Science and Engineering, Yamaguchi University, 1677-1 Yoshida, Yamaguchi 753-8512, Japan*

(Received April 17, 2006; Accepted September 7, 2006)

This paper proposes a new blind deconvolution method with additional phase spectral constraints for a blurred image. A degradation of an original image is mathematically modeled by a convolution of an original image and a point-spread function (PSF). The proposed method consists of the following three steps: (i) projection onto a complex set satisfying the phase spectral constraint in a frequency space; (ii) minimization of a cost function preserving the constrained phase spectra; and (iii) projection onto an image space satisfying nonnegative and support constraints. This method restores both the original image and the PSF with high accuracy. The effectiveness of the proposed method is verified by applying it to some blind deconvolution problems for digital images, and the experimental results show that the performance is superior to the conventional blind deconvolution methods. © 2006 The Optical Society of Japan

Key words: blind deconvolution, image restoration, phase constraint, gradient method, cost function

1. Introduction

In general, the degradation of the original image is mathematically modeled by a convolution of the original image and the point-spread function (PSF). PSF is a function to blur an image. The problem of retrieving an original image from the blurred image is a kind of image restoration problem. The conventional linear image restoration algorithms usually assume that the PSF is known beforehand.[1–7] In many practical situations, however, the PSF is unknown and little can be known about the original image. Therefore, the conventional linear image restoration techniques are not applicable for these practical cases. A blind deconvolution has been proposed to treat these cases.[8–13] The objective of a blind deconvolution is to estimate a PSF and to retrieve an original image from a blurred image, using only *a-priori* information on support of the image and the nonnegativity of a pixel value.

Ayers and Dainty's algorithm (A–D algorithm) is one of the useful methods for a blind deconvolution.[14,15] This algorithm retrieves an original image and at the same time estimates a PSF by iteratively applying an inverse filter under constraints of support of the image and the nonnegativity of a pixel value. This algorithm is often applied to many blind deconvolution problems due to its low computational complexity. However, its convergence property is uncertain. Furthermore, the algorithm is sensitive to initial values and, what is worse, is often unstable.

In order to improve the convergence property of an iterative algorithm, a cost function and a gradient method have been brought into its iterative procedure.[16–18] This algorithm now has a stable convergence property, however, it tends to be trapped at local minima.

There is also a zero-sheet separation method.[19] Good restoration results are obtained, but its algorithm is very complicated and requires high computational cost; thus it is not suited for real-time processing.

In this paper, we propose a gradient-based blind deconvolution method with additional constraints in order to improve restoration performance. The additional constraints are phase spectra of the original image and of the PSF. Those are obtained by Takajo's technique,[20] which is one of the phase retrieval methods[21–24] and can acquire each phase spectrum from the observed image without any additional information.

The effectiveness of the proposed method is verified by applying it to blind deconvolution problems for digital images.

2. Blind Deconvolution and Conventional Method

Here, we first briefly summarize a conventional blind deconvolution based on a gradient method.

A blurred image $g(x, y)$ is represented by a convolution of an original image $f(x, y)$ and a PSF $h(x, y)$ as follows:

$$g(x, y) = \sum_{x'} \sum_{y'} h(x - x', y - y') f(x', y'), \tag{1}$$

where (x, y) is a coordinate in image space. $f(x, y)$ and $h(x, y)$ are real and nonnegative. $G(u, v)$, Fourier transform of $g(x, y)$, is given by:

$$G(u, v) = H(u, v)F(u, v), \tag{2}$$

where $H(u, v)$ and $F(u, v)$ are Fourier transforms of $h(x, y)$ and $f(x, y)$, respectively.

If a PSF is known in advance, the original image is restored by using an inverse filter or Wiener filter.[25] In many cases, however, the PSF is unknown. A blind deconvolution is intended to retrieve the original image from the blurred image without any knowledge of the PSF.

The conventional gradient-based method consists of the iterative steps. Those are minimization of a cost function, and a projection onto an image space satisfying nonnegative

*E-mail address: suetake@sci.yamaguchi-u.ac.jp

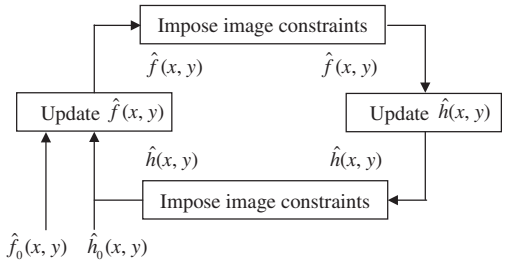

Fig. 1. Block diagram of a gradient-based method. $\hat{f}_0$ and $\hat{h}_0$ are initial estimates. $\hat{f}(x, y)$ and $\hat{h}(x, y)$ are an estimated image and a PSF, respectively. These procedures are repeated until the estimates converge.

and support constraints. Figure 1 shows a block diagram of this method.

In the minimization of the cost function, $\hat{f}(x, y)$ is adjusted to minimize the following cost function in a frequency space:

$$E = \sum_{u,v} \left| G(u, v) - \hat{H}(u, v)\hat{F}(u, v) \right|^2, \tag{3}$$

where $\hat{H}(u, v)$ and $\hat{F}(u, v)$ are Fourier transforms of the estimated $\hat{f}(x, y)$ and $\hat{h}(x, y)$, respectively. In this method, the gradient descent method is employed for an update of $\hat{f}(x, y)$ as follows:

$$\hat{f}^{\text{new}}(x, y) = \hat{f}^{\text{old}}(x, y) - \alpha_{\hat{f}} \frac{\partial E}{\partial \hat{f}^{\text{old}}(x, y)}, \tag{4}$$

where superscripts "old" and "new" represent the before and after updating. $\alpha_{\hat{f}}$ is a descent parameter.

In the projection onto an image space, $\hat{f}(x, y)$ is updated by imposing nonnegative and support constraints as follows:

$$\hat{f}^{\text{new}}(x, y) = \begin{cases} \hat{f}^{\text{old}}(x, y) & (x, y) \notin \gamma_{\hat{f}} \\ 0 & (x, y) \in \gamma_{\hat{f}} \end{cases}, \tag{5}$$

where $\gamma_{\hat{f}}$ is a set of position vectors in a negative space or outside the support of $\hat{f}(x, y)$.

$\hat{h}(x, y)$ is also updated in the similar manner as $\hat{f}(x, y)$ as shown in Fig. 1. These procedures are iterated until the cost function converges.

Although this algorithm has reasonably low computational complexity and stable convergence property, it tends to be trapped at local minimum solutions and has insufficient accuracy of restoration.

3. Proposed Blind Deconvolution Method

In this section, we propose a new blind deconvolution method. It is based on the gradient descent method, and has additional constraints. Those constraints concern the phase spectra of the original image and of the PSF. The phase spectral information is obtained by applying Takajo's method to the amplitude spectrum of the observed image without any additional observation.

3.1 Acquisition of the phase spectral information

The phase spectral information, which is employed in this paper as the additional constraint, is obtained using Takajo's method. The concept is the same as Lane and Bates's method,[22] which uses an error reduction algorithm (ER algorighm) to obtain the phase spectral information concerning $F(u, v)$ and $H(u, v)$. The ER algorithm gives us one of the following four estimates, $F(u, v)H(u, v)$, $F(u, v)H^*(u, v)$, $F^*(u, v)H(u, v)$ or $F^*(u, v)H^*(u, v)$. In this algorithm, the amplitude spectrum of the blurred image $|G(u, v)|$ is used as the amplitude constraint. Pseudo-random phase distributions are usually used as the initial states of the algorithm.[22] The superscript $*$ stands for a complex conjugate.

Among these four estimates, only $F(u, v)H^*(u, v)$ and $F^*(u, v)H(u, v)$ are valid for the acquisition of the phase spectral information. $F(u, v)H(u, v)$ and $F^*(u, v)H^*(u, v)$ can be easily found and excluded because these are identical with $G(u, v)$ and $G^*(u, v)$, respectively. The algorithm is iteratively executed starting from various initial estimates until $F(u, v)H^*(u, v)$ or $F^*(u, v)H(u, v)$ is obtained.

Let $\hat{G}(u, v)$ be either $F(u, v)H^*(u, v)$ or $F^*(u, v)H(u, v)$. In case $F(u, v)H^*(u, v)$ is obtained, the phase spectral information is extracted as:

$$2\phi_H(u, v) = \tan^{-1}\left(\frac{G(u, v)}{\hat{G}(u, v)}\right), \tag{6}$$

and

$$2\phi_F(u, v) = \tan^{-1}\left(\frac{G(u, v)}{\hat{G}^*(u, v)}\right), \tag{7}$$

where $\phi_H(u, v)$ and $\phi_F(u, v)$ correspond to the true phase spectra of $H(u, v)$ and $F(u, v)$, respectively, with modulo π.

In case $F^*(u, v)H(u, v)$ is obtained, the phase spectral information is extracted as:

$$2\phi_F(u, v) = \tan^{-1}\left(\frac{G(u, v)}{\hat{G}(u, v)}\right), \tag{8}$$

and

$$2\phi_H(u, v) = \tan^{-1}\left(\frac{G(u, v)}{\hat{G}^*(u, v)}\right). \tag{9}$$

However, as is well known, the ER algorithm has a local minimum problem, and thus it cannot retrieve exact $F(u, v)H^*(u, v)$ and $F^*(u, v)H(u, v)$ when trapped at a local minimum. The hybrid input–output algorithm (HIO algorithm) with a small feedback constant is therefore employed in Takajo's method instead of the ER algorithm. Takajo's method can break the local minimum problem to get the global minimum solution. Using Takajo's method, $F(u, v)H^*(u, v)$ and $F^*(u, v)H(u, v)$ are retrieved with high accuracy, and thus phase spectral information is accurately estimated.

3.2 Algorithm of the proposed method

The proposed blind deconvolution algorithm consists of the following three procedures: (i) projection onto a complex set satisfying the phase spectral constraints on a frequency space, (ii) minimization of a cost function preserving the constrained phase spectra, and (iii) projection onto an image space satisfying nonnegative and support constraints.

A block diagram of the proposed method is shown in

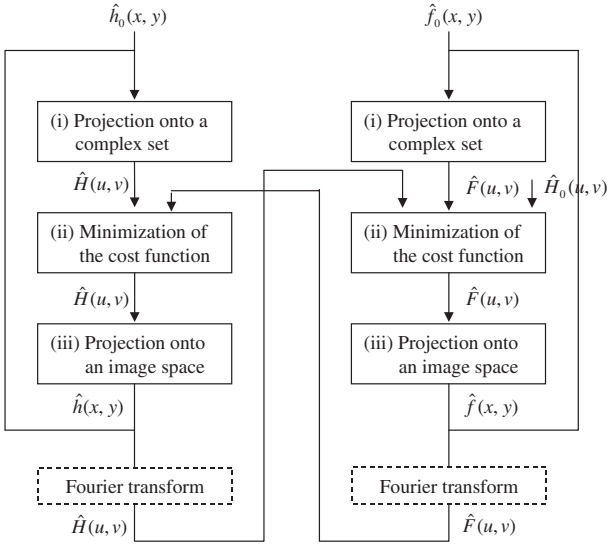

Fig. 2. Block diagram of the proposed method. $\hat{f}_0$ and $\hat{h}_0$ are initial estimates. $\hat{f}(x, y)$ and $\hat{h}(x, y)$ are an estimated image and a PSF, respectively.

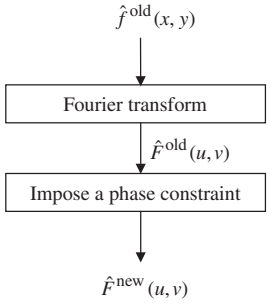

Fig. 3. Block diagram of the projection onto a phase spectral set.

Fig. 2. The right and the left hand parts of the figure show the procedures for updating $\hat{f}(x, y)$ and $\hat{h}(x, y)$, respectively. These sequences are repeated alternately so that the cost function converges.

(i) *Projection onto a complex set*

Figure 3 shows a block diagram of this procedure. In this procedure, $\hat{f}(x, y)$ is transformed to $\hat{F}(u, v)$ by Fourier transform. Then, $\hat{F}(u, v)$ is updated using the additional constraint of the phase spectral information. The updating of $\hat{F}(u, v)$ is achieved by replacing its phase spectrum with the one retrieved by Takajo's method.

The retrieved spectrum $\phi_F(u, v)$ is congruent to a phase spectrum of $F(u, v)$ modulo π.[24] That is, the following relationship holds:

$$\phi_F(u, v) = \theta_F(u, v) \quad \text{or} \quad \theta_F(u, v) - \pi, \tag{10}$$

where $\theta_F(u, v)$ is a phase spectrum of $F(u, v)$. In the proposed method, the phase spectrum is updated by using $\phi_F(u, v)$ or $\phi_F(u, v) + \pi$, as follows:

$$\theta_{\hat{F}}^{\text{new}}(u, v) = \begin{cases} \phi_F(u, v) & (u, v) \in S \\ \phi_F(u, v) + \pi & (u, v) \notin S \end{cases}, \tag{11}$$

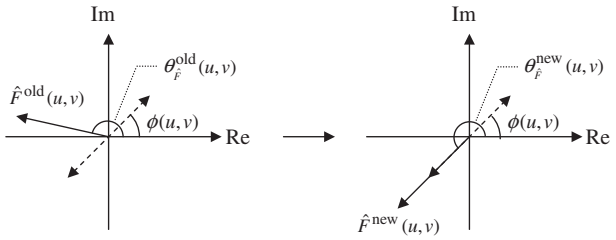

Fig. 4. Geometrical representation of the projection onto a phase spectrum. The solid and dashed vectors represent $\hat{F}(u, v)$ and a unit vector with retrieved phase spectrum, respectively. The left and right hand parts of the figure stand for the situations before and after updating, respectively.

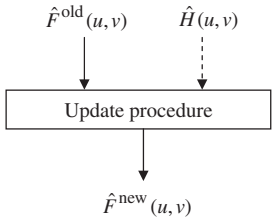

Fig. 5. Block diagram of the minimization of the cost function.

with

$$S = \{(u, v) | d_1(u, v) \leqq d_2(u, v)\}, \tag{12}$$

$$d_1(u, v) = \theta_{\hat{F}}^{\text{old}}(u, v) - \phi_F(u, v), \tag{13}$$

$$d_2(u, v) = \theta_{\hat{F}}^{\text{old}}(u, v) - (\phi_F(u, v) + \pi), \tag{14}$$

where $\theta_{\hat{F}}(u, v)$ is a phase spectrum of $\hat{F}(u, v)$. $d_1(u, v)$ and $d_2(u, v)$ are in the range of $(-\pi, \pi]$. $\hat{F}(u, v)$ is thus updated by using $\theta_{\hat{F}}^{\text{new}}(u, v)$ without changing its amplitude spectrum $|\hat{F}(u, v)|$ as shown in Fig. 4.

(ii) *Minimization of the cost function*

Figure 5 shows a block diagram of this procedure, in which $\hat{F}(u, v)$ is adjusted so that the cost function, defined by eq. (3), is minimized. For minimization of the cost function, the gradient descent only on the amplitude spectrum is applied to preserve the phase spectrum already constrained in the previous procedure.

The following is an updating procedure:

$$\left|\hat{F}^{\text{new}}(u, v)\right| = \left|\hat{F}^{\text{old}}(u, v)\right| - \alpha_{\hat{F}} \frac{\partial E}{\partial \left|\hat{F}^{\text{old}}(u, v)\right|}, \tag{15}$$

where $\alpha_{\hat{F}}$ is a descent parameter. The gradient of the cost function with respect to $|\hat{F}^{\text{old}}(u, v)|$ is given by:

$$\frac{\partial E}{\partial \left|\hat{F}^{\text{old}}(u, v)\right|} = -2\Re\left[e^{-i\theta_{\hat{F}}(u, v)} \hat{H}^*(u, v) \varepsilon_{\hat{F}}(u, v)\right] \tag{16}$$

with

$$\varepsilon_{\hat{F}}(u, v) = G(u, v) - \hat{F}^{\text{old}}(u, v) \hat{H}(u, v), \tag{17}$$

where $\Re[\cdot]$ stands for a real part of a complex number.

The descent parameter $\alpha_{\hat{F}}$ is determined in order to minimize the cost function. After the updating of $\hat{F}(u, v)$, the cost function becomes:

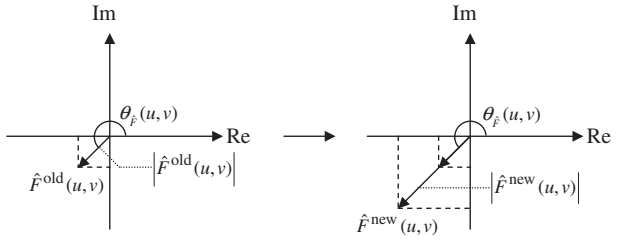

Fig. 6. Geometrical representation of the updating of $\hat{F}(u,v)$. The left and right hand parts of the figure stand for the situations before and after updating, respectively.

$$E_{\hat{F}} = \sum_{u,v} \left| G(u,v) - \left|\hat{F}^{\mathrm{new}}(u,v)\right| e^{i\theta_{\hat{F}}(u,v)} \hat{H}(u,v) \right|^2. \quad (18)$$

$E_{\hat{F}}$ is a quadratic convex function with respect to $\alpha_{\hat{F}}$. Therefore, $\alpha_{\hat{F}}$ minimizing the cost function satisfies the following equation:

$$\frac{\partial E_{\hat{F}}}{\partial \alpha_{\hat{F}}} = 0. \quad (19)$$

Accordingly, $\alpha_{\hat{F}}$ is given by:

$$\alpha_{\hat{F}} = -\frac{\sum_{u,v} \Re\left[e^{-i\theta_{\hat{F}}(u,v)} D_{\hat{F}}(u,v) \hat{H}^*(u,v) \varepsilon_{\hat{F}}(u,v) \right]}{\sum_{u,v} D_{\hat{F}}^2(u,v) \left|\hat{H}(u,v)\right|^2} \quad (20)$$

with

$$D_{\hat{F}}(u,v) = \frac{\partial E}{\partial \left|\hat{F}^{\mathrm{old}}(u,v)\right|}. \quad (21)$$

From a geometrical point of view, this minimization procedure means that $|\hat{F}^{\mathrm{old}}(u,v)|$ is adjusted to minimize the cost function without changing its phase spectrum $\theta_{\hat{F}}(u,v)$ as shown in Fig. 6.

(iii) *Projection onto an image space*

A block diagram of this procedure is shown in Fig. 7. In this procedure, $\hat{f}(x,y)$ is obtained by an inverse Fourier transform of $\hat{F}(u,v)$. $\hat{f}(x,y)$ is also updated by eq. (5) in a similar manner as described in §2.

$\hat{h}(x,y)$ is updated in the same way as $\hat{f}(x,y)$. As shown in Fig. 2, these procedures are alternately iterated until the cost function converges.

4. Experimental Results

In the experiments, the following four kinds of images are employed as original images. As shown in Fig. 8, these are: cropped parts of "Lena," "Barbara," "Building," and "Text" in a standard image database (SIDBA).[26] Each cropped image in SIDBA is constituted of 64×64 pixels. The resolutions of the original images are all 8 bits gray-level in the range of $[0, 1]$.

As the PSFs, four kinds of images shown in Fig. 9 are employed: three typical PSFs of "Disk," "Line," and "Gaussian," and a complex shaped PSF of "Complex," which are constituted of 15×15, 5×7, 6×6, and 7×5 pixels, respectively. Their resolutions are the same as those of the original images. "Disk" and "Line" shaped PSFs are known as models of out-of-focus and motion blur, respectively. A "Gaussian" shaped PSF is a model of atmospheric turbulence.

The observed images employed in the experiments are generated by the convolution of all possible combinations of the four original images and four PSFs. The restoration simulation is executed for all 16 (4×4) kinds of the observed images.

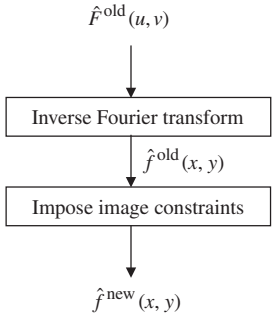

Fig. 7. Block diagram of the projection onto an image space.

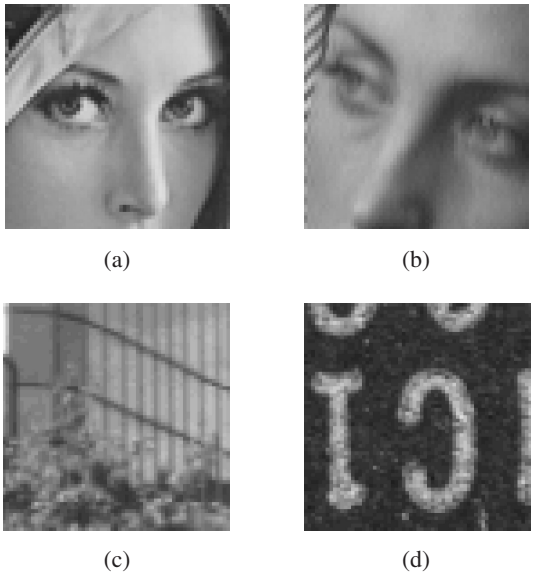

Fig. 8. Original images employed for the experiments. (a) "Lena." (b) "Barbara." (c) "Building." (d) "Text."

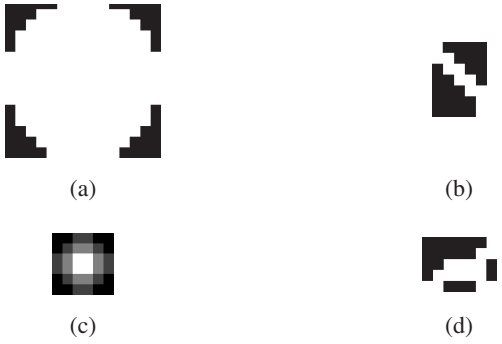

Fig. 9. PSFs employed for the experiments. (a) "Disk." (b) "Line." (c) "Gaussian." (d) "Complex."

Table 1. $RMSE_{\mathrm{P}}$s for all the observed images.

Original image	PSF			
	Disk	Line	Gaussian	Complex
Lena	0.254	0.005	0.512	0.478
Barbara	0.051	0.210	0.157	0.024
Building	0.316	0.013	0.303	0.023
Text	0.295	0.004	0.136	0.138

For a comparison, two typical conventional methods, "A–D algorithm" and "gradient-based method" are used. The restoration performance is evaluated by an average and a standard deviation of root mean squared error (*RMSE*) for some trials to each observed image. *RMSE* is defined by:

$$RMSE = \sqrt{\frac{\sum_{x,y}\left(f(x,y) - \hat{f}(x,y)\right)^2}{N}}, \tag{22}$$

where N stands for the number of pixels of $f(x,y)$.

In the proposed method, the phase spectral information is estimated by using Takajo's method beforehand. The phase estimation performance is evaluated by *RMSE* for the estimated phase spectral information ($RMSE_{\mathrm{P}}$). $RMSE_{\mathrm{P}}$ is defined as:

$$RMSE_{\mathrm{P}} = \sqrt{\frac{\sum_{u,v}\left(\phi_T(u,v) - \phi_F(u,v)\right)^2}{N}}, \tag{23}$$

where $\phi_T(u,v)$ is the true phase spectral information corresponding to $\phi_F(u,v)$. $|\phi_T(u,v) - \phi_F(u,v)|$ is in the range of $[0,\pi]$. For all the experiments, the feedback constant in the HIO algorithm is assigned to 0.2.

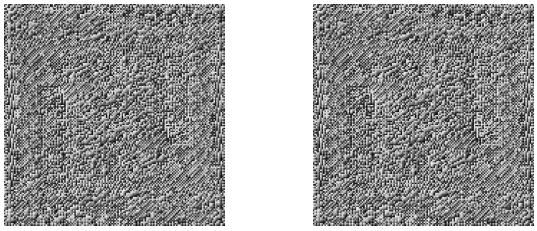

(a) (b)

Fig. 10. Images of phase spectral information for the observed image generated by the convolution of "Barbara" and "Disk." (a) True phase spectral information. (b) Estimated phase spectral information.

$RMSE_{\mathrm{P}}$s for all the observed images are shown in Table 1 and are confirmed to be reasonably small for all the observed images. Furthermore, the images of the true phase spectral information and the estimated one for the observed image, generated by the convolution of "Barbara" and "Disk," are shown in Fig. 10. The phase spectral information is estimated almost perfectly. The estimated phase spectral information is used as the additional constraint of the proposed method.

Ten experimental trials are executed for each observed image with random initial estimates. Averages of *RMSE* are shown in Fig. 11; it is seen that averages of the proposed method are less than those of the conventional methods for all the images. Furthermore, it is also seen that the standard deviations of *RMSE* of the proposed method are sufficiently

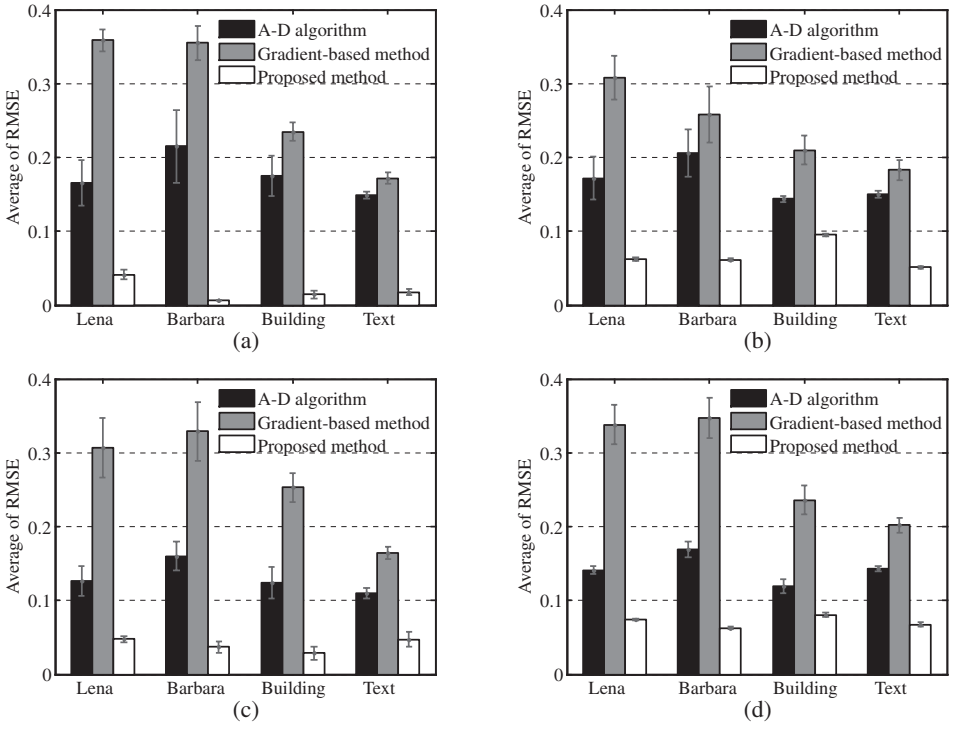

Fig. 11. Averages and standard deviations of *RMSE*. (a), (b), (c), and (d) show the results when PSFs are "Disk," "Line," "Gaussian," and "Complex," respectively.

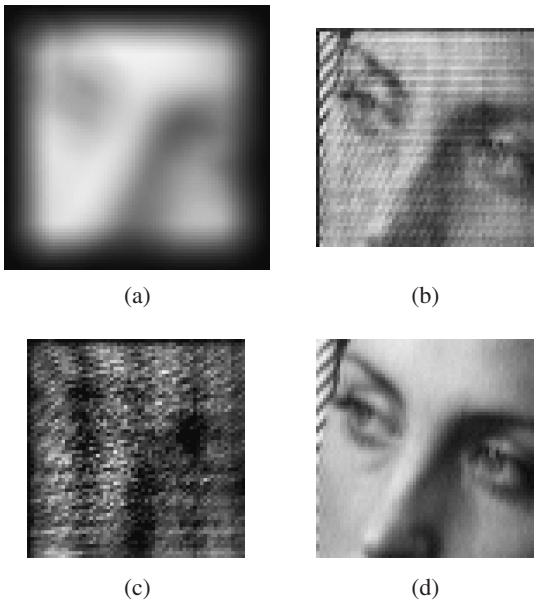

Fig. 12. Examples of restoration results. (a) The observed image generated by the convolution of "Barbara" and "Disk." (b), (c), and (d) are the restored images by the A–D algorithm, the gradient-based method, and the proposed method, respectively.

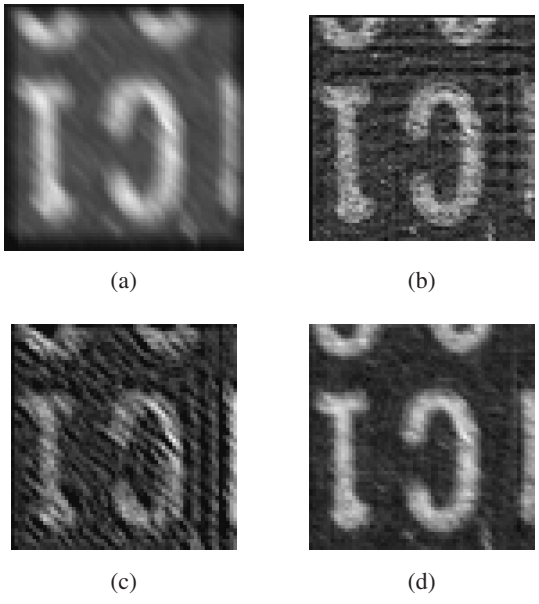

Fig. 13. Examples of restoration results. (a) The observed image generated by the convolution of "Text" and "Line." (b), (c), and (d) are the restored images by the A–D algorithm, the gradient-based method, and the proposed method.

small. These facts make it clear that the proposed method has good and stable restoration performance in comparison with the conventional methods.

Examples of restoration results are shown in Figs. 12 and 13. From them, the superiority of the proposed method is also visually confirmed.

For restoration examples shown in Fig. 12, the normalized costs versus iterations are shown in Fig. 14. The normalized

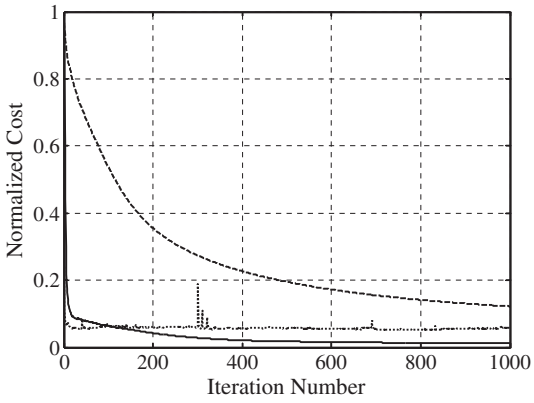

Fig. 14. The normalized cost vs iterations. These results show the restoration processes for the case shown in Fig. 11. The solid, dashed, and dotted lines represent the results of the proposed method, the gradient-based method, and the A–D algorithm, respectively.

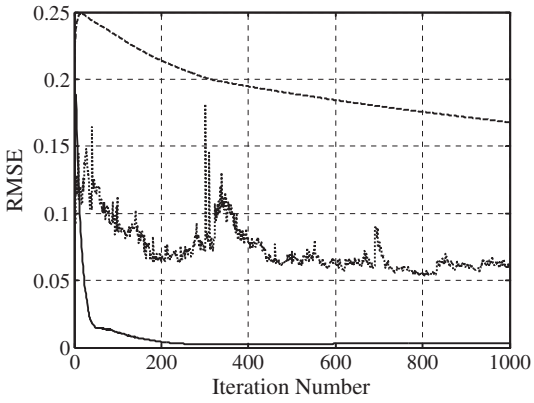

Fig. 15. *RMSE* vs iterations. These results show the restoration processes for the case shown in Fig. 11. The solid, dashed, and dotted lines represent the results of the proposed method, the gradient-based method, and the A–D algorithm, respectively.

cost *NC* is defined by:

$$NC = \frac{\sum_{u,v} \left| G(u,v) - \hat{F}(u,v)\hat{H}(u,v) \right|}{\sum_{u,v} \left| \hat{F}(u,v) \right| \left| \hat{H}(u,v) \right|}. \tag{24}$$

In Fig. 14, the solid, dashed, and dotted lines show the results of the proposed method, gradient-based method, and A–D algorithm, respectively. It is observed that the normalized cost of both the proposed method and the gradient-based method converge, although the cost of the A–D algorithm fluctuates. Furthermore, the final cost of the proposed method is lower than other methods.

*RMSE*s of the examples shown in Fig. 12 versus iterations are shown in Fig. 15. The meanings of the lines are the same as in Fig. 14. The error of the proposed method converges quickly to minimum value; furthermore, it is far smaller than other methods. Thus, restoration accuracy of the proposed method is superior.

5. Conclusions

In this paper a new blind deconvolution method based on a gradient method with a phase spectral constraint has been proposed. The proposed method consists of the following three procedures: (i) projection onto a complex set, (ii) minimization of a cost function, and (iii) projection onto an image space. Procedure (i) restricts the solution set to satisfy the phase spectral information. Procedure (ii) minimizes the cost function and carries on the convergence property of the gradient-based method. Procedure (iii) restricts the solution set to satisfy the nonnegative and support constraints.

The normalized cost and *RMSE* converged reasonably quickly for the proposed method. Furthermore, the restoration performance of this method was far superior to those of A–D algorithm and gradient-based method. Experimental results suggest that the phase spectral constraint works efficiently.

Future plans involve removing the support constraint and investigating the noise robustness in order to increase the practicality of the proposed method.

References

1) D. B. Gennery: J. Opt. Soc. Am. **63** (1973) 1571.
2) M. Cannon: IEEE Trans. Acoust., Speech, Sig. Proc. **24** (1976) 58.
3) P. Nisenson and R. Barakat: J. Opt. Soc. Am. A **4** (1991) 2249.
4) H. C. Andrews and B. R. Hunt: *Digital Image Restoration* (Prentice Hall, New York, 1997).
5) W. H. Richardson: J. Opt. Soc. Am. **62** (1972) 55.
6) L. B. Lucy: Astron. J. **79** (1974) 745.
7) L. I. Rudin, S. Osher and E. Fatemi: Physica D **60** (1992) 259.
8) D. Kunder and D. Hatzinakos: IEEE Sig. Proc. Mag. **13** (1996) 43.
9) D. Kundur: IEEE Trans. Sig. Proc. **46** (1998) 375.
10) M. Matsuyama, Y. Tanji and M. Tanaka: Proc. IEEE Int. Symp. Circuits and Systems, Geneva, 2000, p. IV-553.
11) D. C. Ghiglia, L. A. Romero and G. A. Mastin: J. Opt. Soc. Am. A **10** (1993) 1024.
12) P. Premaratne and M. Premaratne: Proc. Conf. Convergent Technologies Asia Pacific Region, Bangalore, 2003, p. 6.
13) B. C. McCallum: Opt. Commun. **75** (1990) 101.
14) G. R. Ayers and J. C. Dainty: Opt. Lett. **16** (1988) 547.
15) B. L. K. Davey, R. G. Lane and R. H. T. Bates: Opt. Commun. **69** (1988) 353.
16) R. G. Lane: J. Opt. Soc. Am. A **9** (1992) 1508.
17) H. Takajo, T. Takahashi and A. Hayashi: Kogaku **31** (2002) 169 [in Japanese].
18) T. Takahashi and H. Takajo: Proc. 3rd Int. Symp. Signal Processing Information Technology, Darmstadt, 2003, TP4-6.
19) R. G. Lane and R. H. T. Bates: J. Opt. Soc. Am. A **4** (1987) 180.
20) H. Takajo and T. Takahashi: Kogaku **22** (1993) 419 [in Japanese].
21) J. R. Fienup: Appl. Opt. **21** (1982) 2758.
22) R. G. Lane and R. H. T. Bates: Opt. Commun. **63** (1987) 11.
23) R. G. Lane: J. Mod. Opt. **38** (1991) 1797.
24) T. Takahashi and H. Takajo: Kogaku **21** (1992) 485 [in Japanese].
25) A. Papoulis and S. U. Pillai: in *Probability, Random Variables and Stochastic Process*, ed. C. F. Shultz and M. L. Flomenhoft (McGraw-Hill Higher Education, New York, 2002) 4th ed., Part II, Chap. 13, p. 592.
26) M. Sakauchi, Y. Ohsawa, M. Sone and M. Onoe: IETJ Tech. Rep. **8** (1984) 7 [in Japanese].